

**SEAWEED ALLELOPATHY AGAINST CORAL: SURFACE
DISTRIBUTION OF SEAWEED SECONDARY METABOLITES BY
IMAGING MASS SPECTROMETRY**

A Thesis
Presented to
The Academic Faculty

by

Tiffany Andras

In Partial Fulfillment
of the Requirements for the Degree
Masters of Science in the
School of Biology

Georgia Institute of Technology
July 2012

COPYRIGHT BY TIFFANY ANDRAS

**SEAWEED ALLELOPATHY AGAINST CORAL: SURFACE
DISTRIBUTION OF SEAWEED SECONDARY METABOLITES BY
IMAGING MASS SPECTROMETRY**

Approved by:

Dr. Mark Hay, Advisor
School of Biology
Georgia Institute of Technology

Dr. Facundo Fernandez
School of Chemistry and Biochemistry
Georgia Institute of Technology

Dr. Marc Weissburg
School of Biology
Georgia Institute of Technology

Date Approved: May 16, 2012

[To the students of the Georgia Institute of Technology]

ACKNOWLEDGEMENTS

I would like to thank first and foremost my mother, who has been my beacon of strength and integrity and an unwavering source of guidance throughout my academic career. To my father, thank you for being a role model of work ethic and commitment to success. I wish to especially express my overwhelming gratitude to Cami, who gave me the empowerment to persevere. I would also like to thank her for putting up with the long hours in the lab and the emotional rollercoaster I must have been throughout this process. I want to thank Mr. Hal Midgette, who sparked my interest in science and put me on the path that led to this work. Finally, I have to thank all the wonderful people at the Georgia Institute of Technology who helped me countless times with advice, questions, problems, methods, and writing. Thank you to my advisor Dr. Mark Hay, Claire Dell, Tiffany Stephens, Stina Jakobbson, Sebastian Engel, Asiri Galhena, Troy Alexander, Rachel Bennett, Joel Keelor, Dr. Facundo Fernandez, Dr. Marc Weissburg, Dr. Doug Rasher, Dr. Margret Teasdale, Dr. Julia Kubanek, Dr. Linda Green, Kevin Roman, and Dr. Mitchell Parry.

TABLE OF CONTENTS

	Page
ACKNOWLEDGEMENTS	iv
LIST OF FIGURES	vii
LIST OF SYMBOLS AND ABBREVIATIONS	viii
SUMMARY	ix
<u>CHAPTER</u>	
1 INTRODUCTION	1
2 METHODS AND MATERIALS	5
Experimental Design	5
Allelochemical Extraction and Isolation	6
Allelochemical Bioassays	7
Desorption Electrospray Ionization Mass Spectrometry (DESI-MS)	8
Statistics	10
3 RESULTS	12
Whole Algal Pairings	12
Allelochemical Pairings	12
Desorption Electrospray Ionization Mass Spectrometry (DESI-MS)	14
4 DISCUSSION	16
5 FIGURES	22
APPENDIX A: SUPPLEMENTAL FIGURES	27
REFERENCES	29
VITA	37

LIST OF FIGURES

	Page
Figure 1: Effects of contact with whole algae (A) and crude algal extracts (B) on natural colonies of <i>P. rus</i> (N = 9).	20
Figure 2: Effects of contact with chemical extracts of <i>P. neurymenioides</i> on natural colonies of <i>P. rus</i> (N = 10).	21
Figure 3: Identification of Neurymenolides from extracts of <i>P. neurymenioides</i> .	22
Figure 4: Concentration of Neurymenolide A on large blades of <i>P. neurymenioides</i> .	23
Figure 5: A heat-map of the concentration of Neurymenolide A and its oxidative degradation products on the surface of small blades of <i>P. neurymenioides</i> .	24
Supplemental Figure 1: Neurymenolide A standard intensity and concentration curves.	25
Supplemental Figure 2: LC-MS comparison of chemical constituents of the chloroform and hexane solvent partitions of crude extract from <i>P. neurymenioides</i> .	26

LIST OF SYMBOLS AND ABBREVIATIONS

*	p < 0.05
DESI-MS	Desorption Electrospray Ionization Mass Spectrometry
PAM	Pulse Amplitude-Modulated
m/z	mass-to-charge ratio
LC-MS	Liquid-Chromatography Mass Spectrometry
HPLC	High Pressure Liquid-Chromatography
ESI	Electrospray Ionization
TOF	Time-of-flight Mass Spectrometer

SUMMARY

Coral reefs are in global decline, with seaweeds increasing as corals decrease. Though seaweeds have been shown to inhibit coral growth, recruitment, and survivorship, the mechanism of these interactions is poorly known. Here we use field experiments to show that contact with four common seaweeds induces bleaching on natural colonies of *Porites rus*. Controls in contact with inert, plastic mimics of seaweeds did not bleach, suggesting treatment effects resulted from allelopathy rather than shading, abrasion, or physical contact. Bioassay-guided fractionation of the hydrophobic extract from the red alga *Phacelocarpus neurymenioides* revealed a previously characterized antibacterial metabolite, Neurymenolide A, as the main allelopathic agent. For allelopathy of lipid soluble metabolites to be effective, the metabolites would need to be deployed on algal surfaces where they could transfer to corals on contact. We used desorption electrospray ionization mass spectrometry (DESI-MS) to visualize and quantify Neurymenolide A on the surface of *P. neurymenioides* and found the metabolite on all surfaces analyzed. The highest concentrations of Neurymenolide A were on basal portions of blades where the plant is most likely to contact other benthic competitors.

CHAPTER 1

INTRODUCTION

Coral reefs are in global decline with seaweeds commonly replacing corals. Throughout the Caribbean, cover of live coral has declined by 80% (Gardner et al., 2003), while declines along the Great Barrier Reef in the Pacific have been nearly 50% (Bellwood et al., 2004). As corals decline, there is often a correlated increase in seaweed cover, with numerous reefs being transformed from a coral-dominated, seaweed-scarce system to coral-depauperate, seaweed-abundant systems (Mumby, 2009). Many factors have been implicated in this phase shift to algal domination (Hughes, 1994; McManus and Poisenberg, 2004; Mumby and Steneck, 2008) including overfishing (Burkepile and Hay, 2006; Hughes et al., 2007), coral bleaching (Ostrander et al., 2000), disease (Aronson and Precht, 2001), ocean acidification (Hoegh-Guldberg et al., 2007), changing nutrient dynamics (Leichter et al., 2003), and local physical disturbances (Rogers and Miller, 2006). Despite many studies having investigated the factors leading to coral decline and macroalgal increases, fewer have focused on the interactions that may maintain reefs in their degraded state and even fewer have explored the mechanism of these interactions.

As a result of coral to seaweed phase-shifts, corals at all life-history stages will more frequently interact with seaweeds. Established algal communities on degraded reefs have been shown to inhibit settlement and survival of coral larvae (Birrell et al., 2008a; Paul et al., 2011), suppress juvenile growth and survival (Box and Mumby, 2007), and diminish cover and survivorship of established corals (Lewis, 1986; Burkepile and

Hay, 2008) creating a negative feedback that sustains reefs in their coral-depauperate states (Birrell et al., 2008b; Mumby and Steneck, 2008). In addition to documenting outcomes of seaweed-coral interactions, recent studies have suggested that mechanisms of coral decline may be chemical and microbial in nature, with an array of seaweeds and their lipid metabolites causing localized bleaching and death (Rasher and Hay, 2010; Rasher et al., 2011) as well as inducing disease in a variety of coral species (Nugues et al., 2004; Smith et al., 2006; Barott et al., 2011). These results suggest that contact between algae and corals may play a significant role in enhancing coral loss and suppressing coral recovery, and that these negative interactions could be chemically mediated.

If seaweeds are transferring toxic lipids or acting as vectors of microbial pathogens to corals, then critical interactions between seaweeds and corals will be occurring directly on or between organism surfaces. Surfaces represent an important site of ecological interaction serving as the first point of contact between two organisms and as the first line of defense in aquatic environments where organisms are constantly in contact with millions of microbial cells (Steinberg et al., 1997; Steingberg and deNys, 2002). In the case of coral-algal competition, allelopathic metabolites that cause damage limited to sites of contact are lipid-soluble (Rasher and Hay, 2010; Rasher et al., 2011) and would therefore need to be deployed on algal surfaces where they could transfer to corals on contact. Though previous studies have suggested surface deployment of some seaweed secondary metabolites, until recently, rigorous methods to investigate undamaged biotic surfaces in aquatic systems have remained elusive, with the majority of studies employing the “swab” or hexane “dip” methods (Schmitt et al. 1995, Nylund et

al., 2005; Brock et al., 2007; Nylund et al., 2010). Although these techniques are valuable for suggesting localization of compounds to surfaces, their efficacy in providing a detailed picture of the relative distribution and concentration of compounds on the surface can be questioned. As well, despite that studies using these methods verify cell membranes to be intact after extraction or swabbing of compounds from seaweed surfaces, it is not certain that some metabolites from within cells would not be acquired without cell membrane lysis. In fact, some studies have used solvents such as methanol in addition to hexanes (Saha et al., 2011), and this solvent that is miscible with water would be expected, when tissue is soaked or swabbed, to penetrate cell membranes and make internal metabolites more available to extraction. Therefore, though these physical methods of exploring the surfaces of marine organisms have been productive, a method of evaluating metabolites on biotic surfaces without mechanically contacting the cell surface with swabs would be more desirable.

Recent developments in imaging mass spectrometry allow chemical investigation of natural surfaces under ambient conditions (Nyadong et al., 2009, Esquenazi et al., 2009). Desorption electrospray ionization mass spectrometry (DESI-MS) has been used to localize and quantify metabolites on the surfaces of seaweeds (Lane et al., 2009), suggesting this technique's utility in elucidating presence and concentrations of allelopathic metabolites suspected to be deployed on seaweed surfaces. Here we show, based on field studies with established coral colonies, that Neurymenolide A from the red alga *Phacelocarpus neurymenioides* is allelopathic to the coral. DESI-MS was used to evaluate the presence, location, and approximate concentration of Neurymenolide A on the surface of live *P. neurymenioides*. This study confirms that direct contact with

seaweeds can damage coral, that the allelopathic metabolite occurs on the alga's surface, and that chemical interactions at surface contacts produce these damaging effects on corals. Because Neurymenolide A was first identified as an antibacterial metabolite (Stout et al., 2009), it also suggests multiple roles for deterrent compounds (Schmitt et al., 1995; Kubanek et al., 2002) located on eukaryotic surfaces where contact with multiple natural enemies (pathogens, competitors, consumers) will first occur, and suggests that these allelopathic metabolites could act by destabilizing the coral's microbiome by suppressing beneficial microbes, enhancing detrimental ones, or both (Ritchie, 2006; Smith et al. 2006).

CHAPTER 2

MATERIALS AND METHODS

Experimental Design

To test the effects of whole algal thalli, as well as algal extracts, on coral health, we used natural colonies of *Porites rus* growing at depths of 5-10 m on Votua Reef, Viti Levu, Fiji (18°13.049'S, 177°42.968'E). This coral was selected because it is a) abundant at the study site, b) a branching coral making simultaneous comparison of multiple treatments on different branches of the same colony possible (thus controlling for genotype), and c) naturally found adjacent to a variety of algae making the study of interactions with seaweeds ecologically relevant. Ten to 12 colonies that showed no signs of bleaching and had numerous upright branches were chosen and marked with a numbered tag. Four common macrophytes: the red algae *Callophycus densus*, *Phacelocarpus neurymenioides*, and *Plocamium pacificum*, and the green alga *Rhiphilia pencilloides* were collected from Votua Reef at depths of 5-25 m and attached directly to corals within one day of collection by securing the base of the alga to the middle of a coral branch with a small cable tie. A plastic aquarium plant was also attached to each colony to control for shading, abrasion, and the pressure of the cable tie. All treatments (i.e. the four algae plus control) were blocked by coral colony using ten separate colonies each with all five treatments. Damage to each coral branch was assessed after seven days by visually assigning each treatment branch to one of four levels of bleaching: not bleached (=0), slightly bleached (obvious lighter coloration in the area of contact, but the tissue did not yet appear completely white and possibly dead = 1), a white, "bleached

spot” that was less than the total area contacted by the alga (2), or bleached, with much of the area in contact being white (3). We had intended to assess effects on coral health using Pulse Amplitude-Modulated (PAM) Fluorometry as well as visual assessments, but an instrumental error compromised readings for this part of the experiment. However visual evaluation of bleaching is strongly correlated with assessments of photosynthetic efficiency as measured by PAM (Rasher and Hay, 2010; Rasher et al., 2011).

Allelochemical Extraction and Isolation

All seaweeds bleached corals in areas of contact, but because a larger goal was to rigorously evaluate the surface presence of allelopathic metabolites on seaweeds, we chose to conduct follow-up bioassays only on seaweeds most amenable to surface analysis using DESI-MS. DESI-MS requires a relatively robust and planar surface that can withstand the nebulizing gas impact required for DESI imaging as well as a relatively flat surface so that peak intensities on the mass spectra will not be affected by variation in surface height. This restricted further assays to *C. densus* and *P. neurymenioides* because these species were broad, clean, and rigid enough to be good candidates for DESI-MS investigations of surface metabolites.

Crude extracts from 100 ml volumes of each of these algae were obtained using 100% MeOH (x6 and combined). These were dried *in vacuo*, partitioned between water and ethyl acetate, and the ethyl acetate portion retained, dried *in vacuo*, and their effect on corals tested using methods of Rasher and Hay (2010). For each bioassay a 10 ml equivalent of extract from each alga was resuspended in 500 μ L of methanol and added to 1.96 grams of Phytigel (Sigma-Aldrich, USA) and 9.5 ml of water which was poured over window screen to form 1 cm² squares containing extract. Control gel strips were

made in an identical way, but contained only the solvent. Strips were attached to corals by wrapping them around a coral upright and fastening this loosely with a cable tie. Treatments were again blocked by colony so that each colony (N = 12) contained a strip with the extract from each alga and a control strip. Coral health was assessed after 24 h using *in situ* Pulse Amplitude-Modulated (PAM) Fluorometry (Walz, Germany) conducted at the approximate center of each gel strip's contact with the coral upright.

Because initial tests of crude extracts demonstrated more potency of *P. neurymenioides* than *C. densus*, we conducted further bioassay-guided separation experiments with *P. neurymenioides* to separate, purify, and identify the allelopathic metabolites. We extracted an additional 200 ml volume of *P. neurymenioides* with 100% MeOH (x3 and combined) followed by 50:50 MeOH: dichloromethane (x4 and combined). This crude extract was then liquid-liquid partitioned between equal volumes of hexane and 9:1 MeOH: H₂O and both portions were dried. The 9:1 MeOH: H₂O portion was further fractionated by partitioning with equal volumes of chloroform and 3:2 MeOH: H₂O and again dried. The active chloroform partition was further fractionated using silicate bench-top chromatography. 160 g of silica gel was loaded (12 cm) into an 18 cm x 7 cm glass column (total volume = 692.72 cm³) followed by a thin layer of sand (VWR, Lot #: 89872). One hundred fractions were generated using 400 ml of solvent at a gradient of 100, 80, 50, 20, 0% hexane with ethyl acetate followed by 94% ethyl acetate 5% MeOH and 1% acetic acid and lastly 93% ethyl acetate 5% MeOH and 2% acetic acid. Fractions were recombined into a total of 6 fractions based on TLC in 70:30 hexane: ethyl acetate and dried *in vacuo*. Fractions produced by all of the above

separations were tested in the field using the gel-based procedures of Rasher and Hay (2010) described above (N=9).

Fractions that decreased effective quantum yield values, as indicated by decreased PAM readings, were analyzed using liquid-chromatography mass-spectrometry (LC-MS) and normal-phase high-performance liquid chromatography (HPLC). All active fractions were found to contain the same prominent peaks: a pair of peaks relating to the diastereomeric atropisomers of Neurymenolide A followed immediately by a single peak of Neurymenolide B (Stout et al., 2009). Accurate identification of compounds was confirmed using a combination of methods including: comparison with known ^1H NMR spectra, retention time on both an LC-MS and HPLC, peak shape on the HPLC, and accurate mass measurements using ESI-TOF MS in positive ion mode.

After demonstrating that neurymenolides were present in fraction 4 from the chloroform partition (generated from the 80% and 50% hexane flushes), we used normal-phase HPLC to produce purified Neurymenolide A, purified Neurymenolide B, and the “remainder” of metabolites in this fraction. HPLC was performed using a gradient of hexanes and ethyl acetate on a 250 nm x 9.4 mm 5 μm RX-SIL Agilent column. Field bioassays of these metabolites and of the “remainder” were conducted as described above (N=10).

Desorption Electrospray Ionization Mass Spectrometry (DESI-MS)

The above assays identified Neurymenolide A as the allelopathic metabolite in *P. neurymenioides*. To evaluate whether Neurymenolide A was present on the surface of *P. neurymenioides* and at what concentrations, living thalli of *P. neurymenioides* were flown from Fiji to Atlanta and held in recirculating aquaria. DESI-MS was performed under

ambient conditions using a living blade immediately after removal from the plant and with no pretreatment. For the evaluation, we used a custom-built DESI ion source (Nyadong et al., 2008) on an LCQ DECA XP+ quadrupole ion trap mass spectrometer (Thermo Finnigan). Experiments were performed using a solvent spray solution of 100 μM NH_4Cl (Sigma–Aldrich) in MeOH at a flow rate of 7 $\mu\text{L}/\text{min}$. The nebulizer gas pressure was set to 120 psi. The ion transfer capillary was held at 300°C, and experiments were performed in negative ion mode. The DESI sprayer emitter was mounted 2 mm above the algal surface at an angle of 55°. Data were collected in full scan mode (m/z 150–500) using Xcalibur software version 2.0 (Thermo Finnigan). The automatic gain control (AGC) was disabled with a fixed ion injection time of 40 ms. Imaging data were acquired in looped stage scanning mode, controlled by LabVIEW software (National Instruments). Samples were scanned shuttle-wise with a scan speed in both dimensions of 160 $\mu\text{m}/\text{s}$ and a step size in the y-dimension of 180 μm . Images were processed with an in-house MATLAB (version R2008a, MathWorks) script.

Metabolite Distribution Across Whole Algal Surface

Analysis of metabolite location across surfaces from different portions of thalli were accomplished by cutting 2 squares of approximately 0.5 cm^2 from the top, middle, and bottom of large (7.0 cm -10.0 cm), individual blades of *P. neurymenioides* (N = 5). Squares were mounted to a slide using fast-drying glue and mass spectral data were collected for the duration of 100 scans per square. The total ionic intensity of Neurymenolide A was summed (using both the $[\text{M}-\text{H}]^-$ and $[\text{M}+\text{Cl}]^-$ signals) within a square and averaged per blade (N = 2) followed by per section (N = 5), producing an average intensity for top, middle, and bottom sections of blades. In order to determine

whether the metabolite was differentially distributed at edges or centers of blades, data were collected from the center, with the midrib avoided, and one side of 4 separate blades (1.0 – 2.5 cm broad blades) for a duration of 50 scans and averaged as above. Analysis of chromatograms and spectra were conducted using QualBrowser software (Thermo).

Imaging data were also collected using algal samples (0.5–2.0 cm length; 0.2–2.0 cm width) taken fresh from seawater tanks and attached, without pretreatment, to a microscope slide with instant adhesive glue. Blades used for these images were small, adventitious branches arising from the midrib of larger blades. Algal cell integrity was verified before and after DESI-MS experiments by evaluation under a light microscope.

Estimation of Surface Concentrations

Surface concentrations of Neurymenolide A were estimated by comparing integrals of natural surface concentrations to a standard curve generated on the same day as images by depositing 5 μ l of four Neurymenolide A solutions of known concentration (1 mM, 100 μ M, 10 μ M, 1 μ M) onto a PTFE substrate. Absolute concentrations of standards were calculated by dividing the total number of moles deposited by the area over which the sample was observed to spread ($r = 2$ mm), resulting in absolute concentrations of 298 pmol/mm² to 0.298 pmol/mm² respectively. The summed ionic intensity value for each concentration of Neurymenolide A was calculated using the method described above for distribution on large blades. Concentration was then plotted as a function of summed intensity in order to estimate concentrations from intensity values on sample surfaces.

Statistics

Whole algal pairings with corals were evaluated using a *paired sign test* for each treatment against the control. A Bonferroni correction setting $\alpha = 0.012$ corrected for using the control value in multiple contrasts (contrasts of control versus treatments for four total comparisons).

Data from all extract-coral pairings were tested using an *ANOVA* blocked by coral colony. Data for the first three experimental pairings adhered to assumptions of a parametric test without transformation and data from the last set of treatments were square root transformed to reach normality. *Post-hoc Tukey tests* were completed for pair-wise comparisons between treatments and against the control. An *ANOVA* blocked by blade contrasted metabolite concentrations on top, middle, and bottom portions of blades. This was followed by *post-hoc Tukey tests*. A *paired T-test* evaluated data from edge versus center sections of blades.

CHAPTER 3

RESULTS

Effects of Live Algae

All four species of algae produced significant levels of coral bleaching when placed in contact with branches of *Porites rus* (N = 9) for seven days in the field (Fig. 1A; $p = <0.001$ to 0.009 for all contrasts; paired sign test each treatment versus the control, $\alpha = 0.012$ to control for multiple comparisons). Levels of bleaching tended to be greater for the red alga *Plocamium pacificum* and the green alga *Rhiphilia penicilloides* than for the red algae *Callophycus densus* and *Phacelocarpus neurymenioides*. Contact with a plastic algal mimic (the control for contact, shading, abrasion, etc.) caused no bleaching. Bleaching for all contrasts occurred only in areas of direct contact. Because *C. densus* and *P. neurymenioides* were morphologically most amenable to DESI-MS analysis, we focused further investigation for possible allelopathy in these species.

Allelochemical Pairings

When crude extracts from *C. densus* and *P. neurymenioides* were bioassayed *in situ* against *P. rus* (N = 12), the extract from *P. neurymenioides* decreased the effective quantum yield (Φ_{PSII}) values of the coral by 41% ($P < 0.01$) in 24h while the extract from *C. densus* had no effect (Fig. 1B; blocked ANOVA $F_{2, 22} = 9.02$, $P < 0.001$ for treatment and $F_{11, 22} = 0.40$, $P = 0.948$ for colony). Visual bleaching beneath extract strips occurred for 10 of 12 *P. neurymenioides* replicates, 2 of 12 *C. densus* replicates, and 0 of 12 control replicates.

The crude extract of *P. neurymenioides* was reassessed along with fractions of the crude extract generated from solvent partitions. The crude extract ($P < 0.001$) and chloroform-soluble fraction of that extract ($P = 0.007$) both significantly decreased effective quantum yield; the hexane and more polar fractions of the crude extract had no significant effects (Fig. 2A; blocked ANOVA $F_{4,32} = 11.38$, $P < 0.001$ for treatment and $F_{8,32} = 3.33$, $P = 0.007$ for colony).

When the active, chloroform-soluble fraction was separated via normal phase chromatography, fraction 4 decreased effective quantum yield by 45% ($P < 0.001$), with all other fractions being inactive (Fig. 2B; blocked ANOVA $F_{5,40} = 10.54$, $P < 0.001$ for treatment and $F_{9,40} = 1.36$, $P = 0.233$ for colony). Preliminary evaluations of both active fractions (chloroform and chloroform F4) were conducted by LC-MS before further purification. Retention times (not shown) and m/z values (Fig. 3A) indicated the presence of neurymenolides in both fractions. From the chloroform F4 fraction, pure neurymenolide A and neurymenolide B were obtained using normal-phase HPLC (Fig. 3B). Purity of both compounds was confirmed using an ESI-TOF mass spectrometer (Fig. 3C).

Tests of the separate components from F4 (blocked ANOVA $F_{3,27} = 13.88$, $P < 0.001$ for treatment and $F_{9,27} = 1.27$, $P = 0.295$ for colony) demonstrated that neurymenolide A was solely responsible for the allelopathic effects of the F4 fraction, suppressing effective quantum yield by 35% ($P < 0.001$; Fig. 2C). Neurymenolide B and “remainder” portions of F4 had no detectable effect.

Desorption Electrospray Ionization Mass Spectrometry (DESI-MS)

Desorption electrospray ionization mass spectrometry (DESI-MS)

conducted on mature blades from *P. neurymenioides* revealed that the older, lower portions of the blades contained surface concentrations of Neurymenolide A that were more than double the concentrations occurring on the top or middle portions (blocked ANOVA $F_{2,8} = 4.91$, $P = 0.041$ for treatment and $F_{4,8} = 1.61$, $P = 0.262$ for blade; Fig. 4A). Concentration did not differ between edges and centers of blades (paired T-test $p = 0.234$; Fig. 4B). DESI-MS imaging was performed on a young, adventitious blade sprouting from the midrib of a mature blade (Fig. 5A). This imaging shows a nearly uniform distribution of Neurymenolide A across the surface of the small blade with a few hotspots of increased concentration (Fig. 5B). The oxidative degradation products of Neurymenolide A were also observed on the surface in an intensity nearly matching that of Neurymenolide A (Fig. 5C). When these compounds are color-coded by class with Neurymenolide A coded pink and the degradation products coded green, an overlay of both images (Fig. 4C) produces a purple color where there is location of both compounds and either a pink or green color when only one of the compounds is present. This overlay shows the location of Neurymenolide A and its degradation product to be similar across the surface.

Peak intensities from DESI-MS images were converted to relative concentration of Neurymenolide A on the surface using a concentration curve (Supplemental Figure 1) generated on the day of imaging. The majority of locations on the surface of *P. neurymenioides* show intensities of Neurymenolide A between $1.5e5$ and $3e5$ giving an average surface concentration of 266 pmol/mm^2 across the surface of small, young blades, which matches the approximate concentrations at the tops and middles of larger

blades. Additionally, however, some locations on the algal surface show intensities of Neurymenolide A upwards of 3×10^5 , corresponding to approximate concentrations of 816 pmol/mm².

CHAPTER 4

DISCUSSION

Contact with all four species of reef algae produced visible bleaching on natural colonies of *Porites rus* growing in the field, while the plastic algal mimic produced no bleaching. The green algae *Rhiphilia penicilloides* and the red algae *Plocamiun pacificum* caused severe bleaching, while the red algae *Phacelocarpus neurymenioides* and *Callophycus densus* caused significant but less severe bleaching (Fig. 1A). In addition, visible patterns of bleaching by algal extracts appear to be related to effects on photosynthesis as crude extract of *P. neurymenioides* caused both higher incidence of bleaching and significantly lower effective quantum yield values than did extracts of *C. densus*. Recent studies have shown several macrophytes to cause bleaching and sometimes death in multiple species of corals (Rasher and Hay, 2010; Rasher and Hay, 2011). Though past studies have focused on interactions on shallow reef-flats utilizing small coral branches, this study yielded similar results using seaweeds typical of deeper waters (3-50 m depths) on deeper-water corals that were not fragmented or displaced from the natural benthos. Given that all four of the seaweeds tested caused bleaching to established coral colonies, that the plastic control plant caused no bleaching, and that even the modest bleaching and 41% decrease in effective quantum yield caused by *P. neurymenioides* was due to allelopathic effects of Neurymenolide A, allelopathic algal-coral interactions appear common in deeper, as well as shallow (Rasher and Hay, 2010; Rasher and Hay, 2011), reef systems. This indicates algal-coral competition, and algal allelopathy in particular, could have a substantial impact on coral decline and on

suppression of coral recovery, especially on modern reefs where corals are less abundant, seaweeds more abundant, and thus seaweed-coral contacts more frequent.

Hydrophobic crude extracts of *P. neurymenioides* reproduced bleaching patterns seen in assays using the whole algae, with bleaching occurring in 10 of 12 replicates in the former and 7 of 9 in the latter (Fig. 1B). Although many bioactive, secondary metabolites have been isolated from *C. densus*, with several of these being strongly antibiotic (Kubanek et al., 2006; Lane et al., 2007), extracts from this alga did not significantly suppress photosynthesis or cause bleaching in corals. It is possible that metabolites from this alga are not allelopathic, or that the heating required to incorporate extracts into gels degraded the bioactive compounds from this alga, but not from *P. neurymenioides* or the numerous other seaweeds tested using these methods (Rasher and Hay, 2010; Rasher et al., 2011).

When the lipid-soluble extract of from *P. neurymenioides* was partitioned and tested in the field, both the crude extract and the chloroform fraction significantly decreased effective quantum yield, and other fractions had no detectable effects. Further fractionation and purification of the active chloroform extract from *P. neurymenioides* indicated that only Neurymenolide A was allelopathic to our test coral (Fig. 2). Neurymenolide A has a clear and potent negative effect on the health of natural colonies of the hard coral *Porites rus* while other fractions of the extract from this seaweed did not. The hexane fraction, though not significantly different from controls, was also not significantly different from the active chloroform fraction (Fig. 2A). Interestingly, both the hexane and chloroform fractions contained compounds of identical masses (Supplemental Figure 2). This intermediate effect of the hexane fraction could therefore

be attributed to the presence of neurymenolides, as they are known to elute in both fractions but in higher concentration in the chloroform fraction (T. Alexander, in prep).

Given that considerable contact between seaweeds and corals occurs on natural reefs following removal of herbivores (Lewis 1986; Hughes et al., 2010), and that this has occurred only in recent years due to overharvest of reef herbivores (Jackson et al. 2001), it seems doubtful that Neurymenolide A was selected for allelopathy against corals. Instead, the large numbers of algal metabolites that suppress herbivores or microbes and the long and important role these enemies have played in seaweed biology (Hay and Fenical, 1988; Engel et al., 2002; Kubanek et al., 2003; Hay 2009) suggests that Neurymenolide A is likely to have evolved due to its protective function against consumers or pathogens, but is now also allelopathic to coral. The potency of Neurymenolide A against methicillin-resistant *Staphylococcus aureus* (MRSA) (Stout et al., 2009), makes an ecological role as an antibacterial defense reasonable. Although the speed and localization of bleaching to areas of direct contact only (see also Rasher and Hay, 2010; Rasher et al. 2011) suggest that these compounds could be acting as direct poisons to corals, it is also possible that they could act by disrupting protective bacteria, or enhancing pathogenic bacteria associated with coral mucus (Ritchie, 2006) as suggested by some previous observations of coral-seaweed interactions (Nugues et al., 2004; Smith et al., 2006; Barott et al., 2011).

Despite previous studies showing seaweeds to be allelopathic to corals, the localization of metabolites and the means of transfer from seaweeds to corals have remained uncertain. Methods such as hexane dipping and physical swabbing of surfaces suggested that allelopathic metabolites occurred on surfaces where they could transfer to

corals; however a better evaluation of surface chemistry improves our understanding of possible mechanisms determining the outcome of seaweed-coral interactions. As DESI-MS imaging allows chemical investigation of natural surfaces undisturbed by manipulations, this study focused further investigations on species for which surface investigations by DESI-MS were possible. Surface chemistry investigations of more damaging seaweeds such as *R. penicilloides* and *P. pacificum* would be desirable, but their delicate (*P. pacificum*) or filamentous (*R. penicilloides*) surfaces make this challenging with DESI-MS. However, patterns of bleaching for these algae versus the plastic control suggest that chemical suppression of coral health occurred for those species as well (Jompa and McCook, 2003; Rasher et al., 2011).

Neurymenolide A was found on all surfaces of *P. neurymenioides* (Fig. 5B). The average concentration on older, bottom portions of blades was more than double the concentration found on younger tissues. Though this may suggest that Neurymenolide A is being sequestered in older tissues in order to defend the most valuable part of the seaweed, it is also possible that the metabolite simply accumulates in tissues over time or is selectively allocated to older tissues as these have experienced longer-term exposure to microbial enemies. In addition to Neurymenolide A, two oxidative degradation compounds were also detected in both extracts and on natural surfaces. The first is produced through non-enzymatic oxidation at C-12 and migration of the double bond between C-12 and C-13 to between C-13 and C-14 ($[M+O-H]^-$ $m/z = 383$) and the second from subsequent dehydration of the first ($[M+O-H_2O-H]^-$ $m/z = 365$, T. Alexander, in prep). These oxidative degradation products occurred in not only similar distribution relative to Neurymenolide A (Fig. 5D) but also in similar intensity on the surface of *P.*

neurymenioides (Fig. 5D), suggesting oxidation may occur rapidly for this metabolite. Though oxidation of compounds is known to occur as a by-product of surface analysis by DESI-MS, peaks for these compounds were not observed when neurymenolide standards were analyzed suggesting the appearance of these compounds on natural surfaces is due to biological oxidation rather than a methodological artifact.

DESI-MS allows chemical investigation of natural surfaces, having the potential to elucidate distribution and concentration of chemicals across whole tissue surfaces. Though some metabolites have been shown to be associated with particular structural features of the organism's surface (Lane et al., 2009), DESI-MS can also reveal these sorts of associations simply by overlaying chemical images onto images of the physical surface. These recent developments in imaging mass spectrometry technology have provided a new stepping-stone in the study of interactions at organism's surfaces. Especially in aquatic environments where organisms are constantly in contact with millions of microbes per milliliter seawater, understanding the roles that chemicals play on biotic surfaces is key to understanding microbe-host, host-epibiont, competitive, and plant-grazer interactions in aquatic systems.

Though debate has continued surrounding the leeching of organic compounds into seawater (Dobretsov et al., 2006), this study conclusively demonstrates that antibacterial and allelopathic metabolites can function when deployed on the surfaces of algae. The bleaching localized to sites of direct contact with algae seen in this as well as prior studies combined with presence of active allelopathic metabolites on the surface of a damaging alga suggest direct contact with algae may be more important to the outcome of algal-coral competition than leeching alone.

In spite of persistent obstacles in reef management, understanding that allelopathic algal-coral interactions occur under direct contact has implications for future reef management. Removal of algal communities in close proximity to established coral colonies should be a focus of reef restoration. Herbivore grazing is a large and consistent means of removing algae from reefs (Lewis, 1986; Hughes et al., 2007; Burkepile and Hay, 2008, 2009), thereby preventing further reef degradation by removing algal competitors and increasing substrate availability for coral recruitment and growth. Reef management might profit from an enhanced understanding of which seaweeds pose the greatest threat to corals, which herbivores most control those seaweeds, and focusing efforts on synergistic strategies of seaweed suppression and herbivore protection in order to best facilitate coral recovery. Given our imperfect knowledge of seaweed-coral interactions at present, a reasonable immediate strategy is to focus on increasing herbivore species richness, which decreases overall algal abundance due to feeding complementarity (Burkepile and Hay, 2008; Rasher and Hay submitted) and aids in the recovery status of reefs (Ledlie et al., 2007).

CHAPTER 5

FIGURES

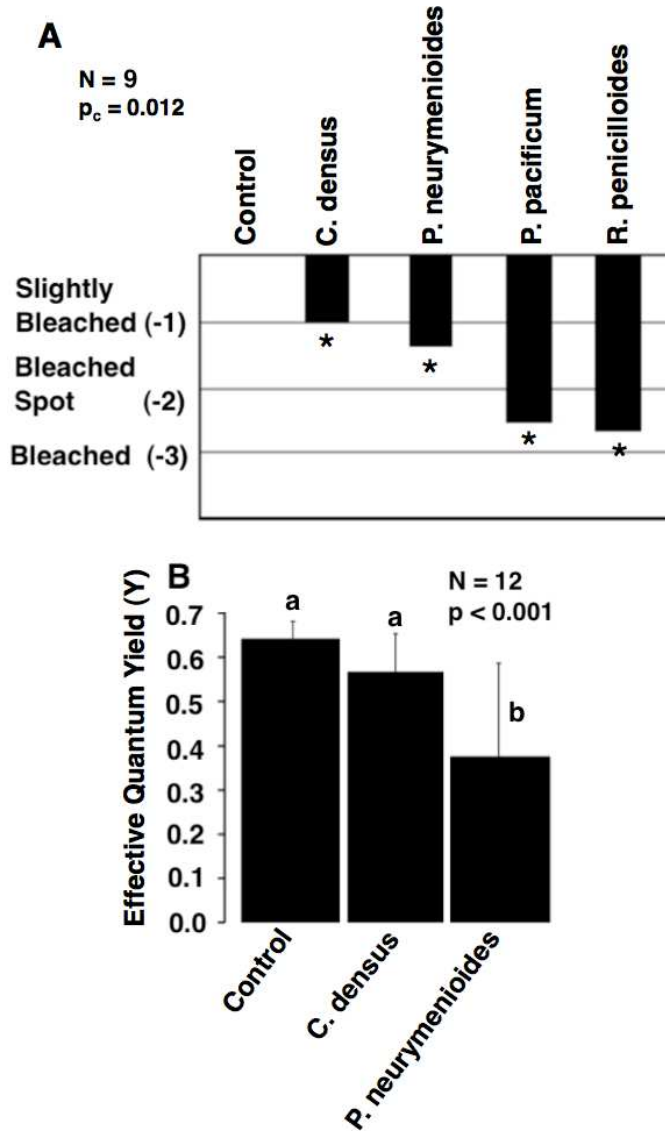


Figure 1: Effects of contact with whole algae (A) and crude algal extracts (B) on natural colonies of *P. rus* (N = 9). Visual data were analyzed using paired sign tests (corrected p_c = 0.012). Photosynthetic efficiency data were analyzed by a blocked ANOVA. Asterisks indicate significant differences (p < 0.05) between treatments and controls, and lowercase letters indicate significant groupings by post-hoc Tukey tests.

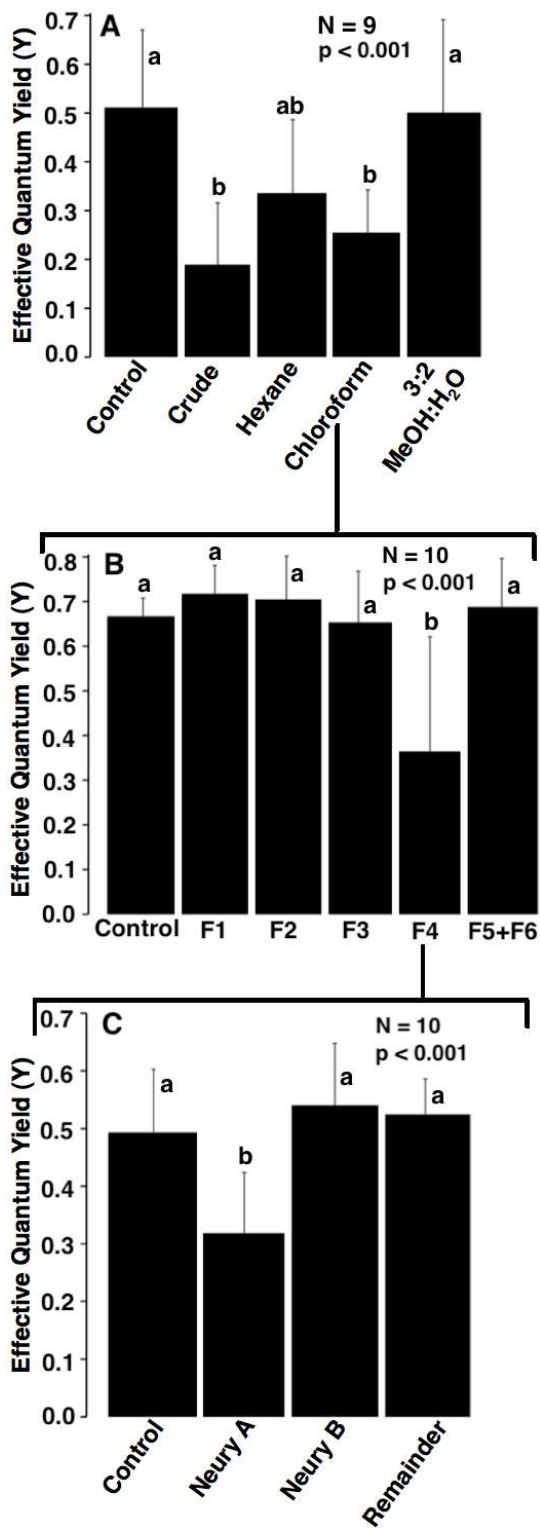


Figure 2: Effects of contact with chemical extracts of *P. neuryenioides* on natural colonies of *P. rus* (N = 10). Bioassay guided fractionation began with testing of the

crude extract and solvent partitions (A). Next, silicate chromatography fractions of the chloroform solvent partition were tested (B) followed finally by purified compounds generated from the F4 chromatography fraction (C). Photosynthetic efficiency data were analyzed by a blocked ANOVA. Lowercase letters indicate significant groupings by post-hoc Tukey tests.

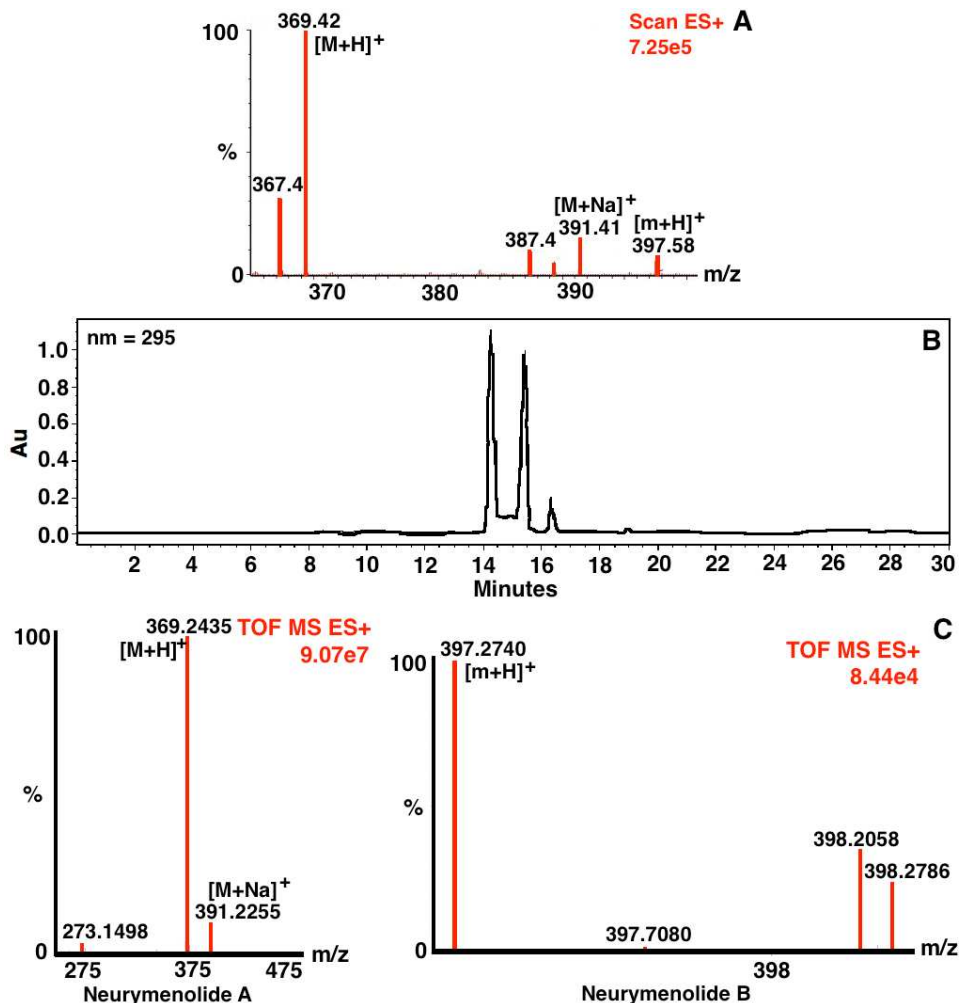


Figure 3: Identification of Neurymenolides from extracts of *P. neurymenioides*.

Compounds were first identified by LC-MS of the chloroform solvent partition, which shows masses matching known values for Neurymenolide A (M) and B (m) (A). HPLC chromatogram from the F4 chromatography fraction showing the two associated peaks of

Neurymenolide A followed by the single peak of Neurymenolide B (B), and accurate mass identification of both compounds using ESI-TOF (C).

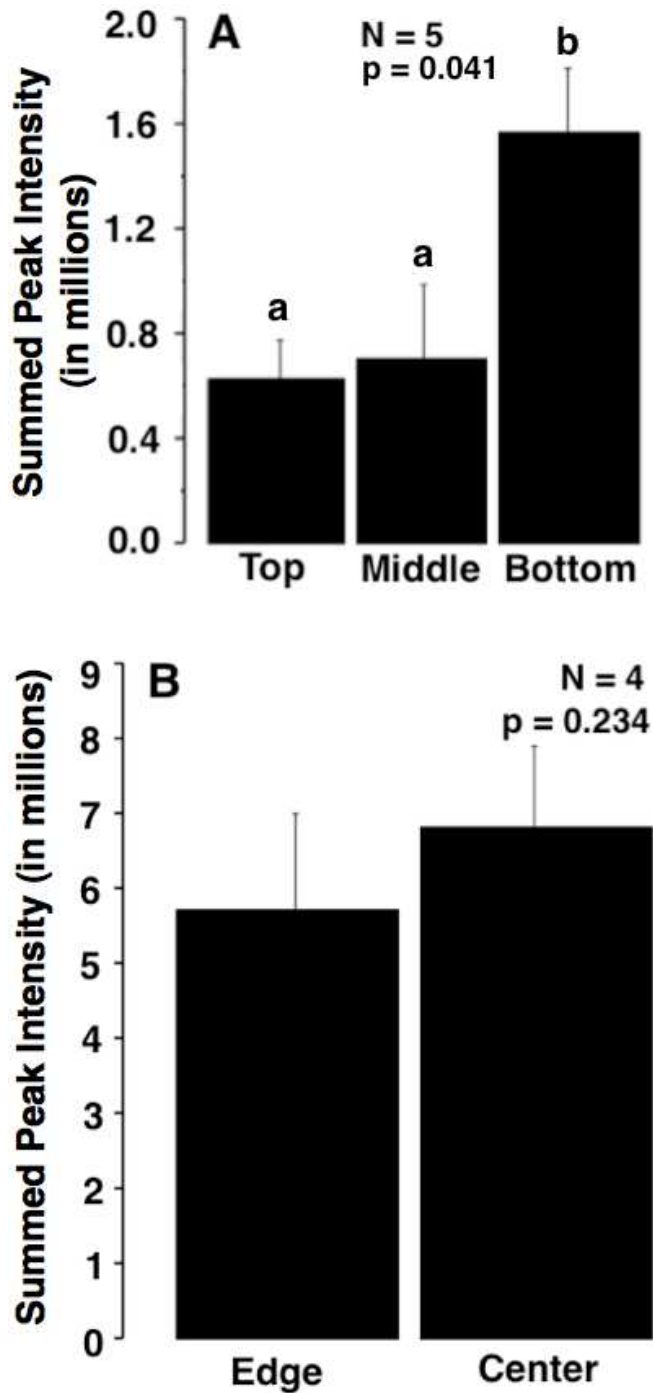


Figure 4: Concentration of Neurymenolide A on large blades of *P. neurymenioides*.

Differences between top, middle, and bottom portions (N = 5) (A) were analyzed using a

repeated measures ANOVA. Edge and center data (N = 4) (B) were compared using a paired T-test. Lowercase letters indicate significant groupings by post-hoc Tukey tests.

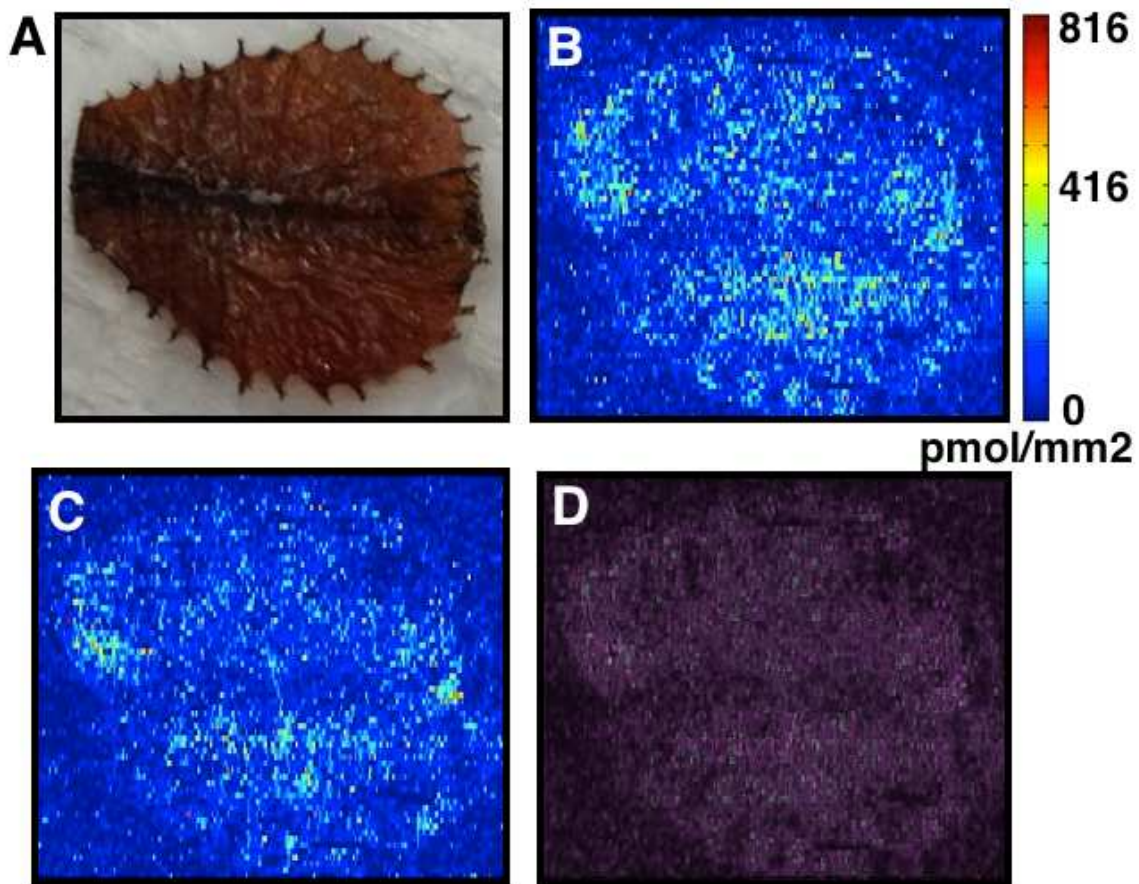
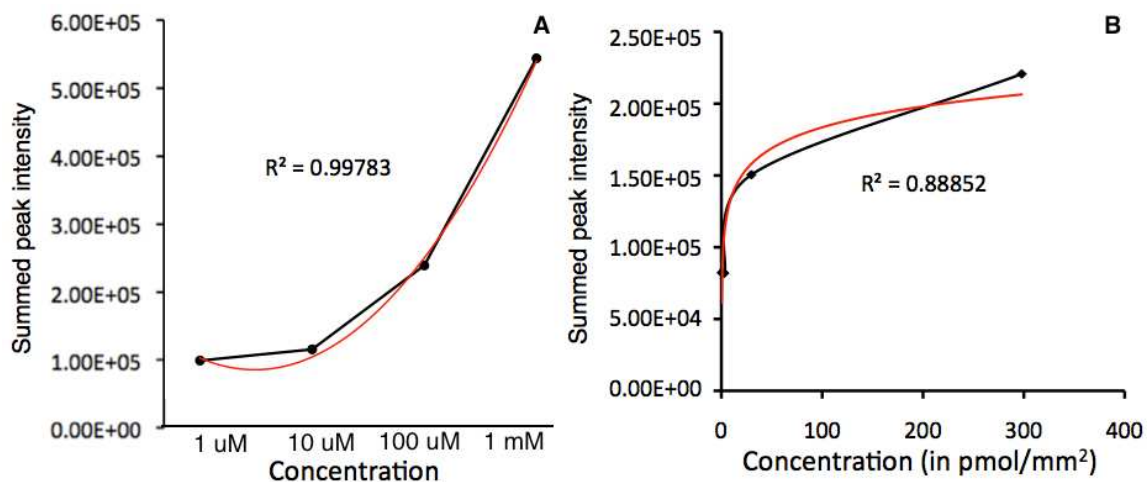


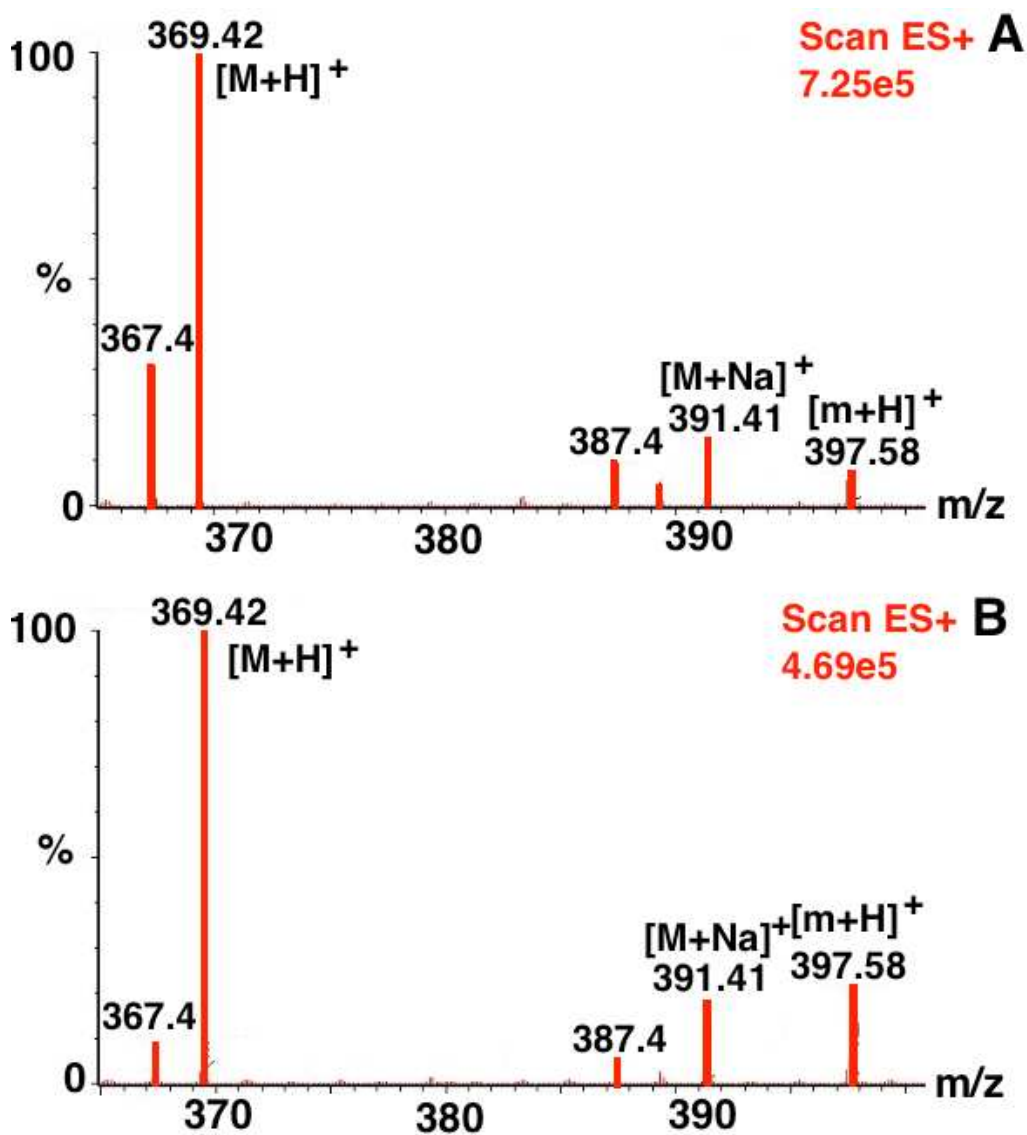
Figure 5: A heat-map of the concentration of Neurymenolide A and its oxidative degradation products on the surface of small blades of *P. neurymenioides*. Mass spectral data was collected using a small, live, untreated blade of *P. neurymenioides* (A). (B) For Neurymenolide A, concentration was determined using a standard concentration curve. (C) For the degradation products the standard curve could not be applied due to possible differences in ionization rates and therefore extrapolations to concentrations could not be made. (D) An overlay of the surface distributions of Neurymenolide A (coded pink) and oxidative degradation products (coded green) is purple at sites of overlap and either pink or green at sites of unique surface association.

APPENDIX A

SUPPLEMENTAL FIGURES



Supplemental Figure 1: Neurymenolide A standard intensity and concentration curves. In order to generate a standard concentration curve 5 μl of standard at four different concentrations was applied in ethyl acetate to a PTFE tablet. (A) The $[\text{M}-\text{H}]^-$ and $[\text{M}+\text{Cl}]^-$ Neurymenolide A ion intensities were summed over 50 scans for each known concentration to generate a standard curve of summed peak intensity as a function of concentration deposited. (B) The concentration of standards was then converted into number of moles of Neurymenolide A per mm^2 area and plotted against the summed peak intensity in order to further estimate concentration of Neurymenolide A on the surface from detected intensities.



Supplemental Figure 2: LC-MS comparison of chemical constituents of the chloroform and hexane solvent partitions of crude extract from *P. neurymenioides*. Masses (m/z) matching known values for neurymenolides were identified in both the chloroform (A) and hexane (B) portions of the crude extract; however, peaks for both Neurymenolide A (M: m/z = 369.42) and Neurymenolide B (m: m/z = 397.58) were found in higher abundance in the chloroform than the hexane fraction (7.25e5 and 4.69e5 respectively).

REFERENCES

Aronson and Precht (2001) White-band disease and the changing face of Caribbean coral reefs *Hydrobiologia* 460: 25-38.

Barott, Rodriguez-Brito, Janouskovec, Marhaver, Smith, Keeling, Rohwer (2011) Microbial diversity associated with four functional groups of benthic reef algae and the reef building coral *Montastrea annularis* *Enviro. Microbio.* 13(5): 1192-1204.

Bellwood, Hughes, Falke, Nystrom (2004) Confronting the coral reef crisis *Nature* 429 (6994): 827-833.

Birrell, McCook, Willis, Harrington (2008a) Chemical effects of macroalgae on larval settlement of the broadcast spawning coral *Acropora millepora* *Mar. Ecol. Prog. Ser.* 362: 129-137.

Birrell, McCook, Willis, Diaz-Pulido (2008b) Effects of benthic algae on the replenishment of corals and the implications for the resilience of coral reefs *Oceanogr. Mar. Biol. Annu. Rev.* 46: 25-64.

Brock, Nylund, Pavia (2007) Chemical inhibition of barnacle larval settlement by the brown alga *Fucus vesiculosus* *Mar. Ecol. Prog. Ser.* 337: 165-174.

Box and Mumby (2007) Effect of macroalgal competition on growth and survival of juvenile Caribbean corals *Mar. Ecol. Prog. Ser.* 342: 139-149.

Burkepile and Hay (2006) Herbivore vs. nutrient control of marine primary producers: context-dependent effects *Ecology* 87(12): 3128-3139.

Burkepile and Hay (2008) Herbivore species richness and feeding complementarity affect community structure and function on a coral reef *Proc. Natl. Acad. Sci. U.S.A* 105:16201-16206.

Burkepile and Hay (2009) Nutrient versus herbivore control of macroalgal community development and coral growth on a Caribbean reef *Mar. Ecol. Prog. Ser.* 389: 71-84.

Dobretsov, Dahms, Harder, Qian (2006) Allelochemical defense against epibiosis in *Caulerpa racemosa* var *turbinata* *Mar. Ecol. Prog. Ser.* 318: 165-175.

Engel, Jensen, Fenical (2002) Chemical ecology of marine microbial defense *J. Chem. Ecol.* 28(10): 1971-1985.

Esquenazi, Dorrestein, Gerwick (2009) Probing marine natural product defenses with DESI-imaging mass spectrometry *Proc. Natl. Acad. Sci. U.S.A* 106(18): 7269-7270.

Gardner, Cote, Gill, Grant, Watkinson (2003) Long-term region-wide declines in Caribbean corals *Science* 301: 958-60.

Hay and Fenical (1988) Marine plant-herbivore interactions: The ecology of chemical defense *Ann. Rev. Ecol. Sys.* 19: 111-145.

Hay (2009) Marine chemical ecology: Chemical signals and cues structure marine populations, communities, and ecosystems *Ann. Rev. Mar. Sci.* 1: 193-212.

Hoegh-Guldberg, Mumby, Hooten, Steneck, Greenfield, Gomez, et al. (2007) Coral reefs under rapid climate change and ocean acidification *Science* 318(5857): 1737-1742.

Hughes (1994) Catastrophies, phase-shifts, and large-scale degradation of a Caribbean coral-reef *Science* 265(5178): 1547-1551.

Hughes, Rodrigues, Bellwood, Ceccarelli, Hoegh-Guldberg, McCook, et al. (2007) Phase shifts, herbivory, and the resilience of coral reefs to climate change *Curr Biol* 17:360–365.

Hughes, Graham, Jackson, Mumby, Steneck (2010) Rising to the challenge of sustaining coral reef resilience *Trends Ecol. Evol.* 25: 633-642.

Jackson, Kirby, Berger, Bjorndal, Botsford, Bourque, et al. (2001) Historical overfishing and the recent collapse of coastal ecosystems *SCIENCE* 293(5530): 629-638.

Jompa, McCook (2003) Coral-algal competition: macroalgae with different properties have different effects on corals *Mar. Ecol. Prog. Ser.* 258: 87–95.

Kubaneck, Whalen, Engel, Kelly, Henkel, Fenical, Pawlik (2002) Multiple defensive roles for triterpene glycosides from two Caribbean sponges *Oecologia* 131: 125–136.

Kubaneck, Jensen, Keirfer, Sullards, Collins, Fenical (2003) Seaweed resistance to microbial attack: A targeted chemical defense against marine fungi *Proc. Natl. Acad. Sci. U.S.A* 100(12): 6916-2921.

Kubaneck, Prusak, Snell, Giese, Fairchild, Aalbersberg, Hay (2006) Bromophycolides C-I from the Fijian red algae *Callophycus densus* *J. Nat. Prod.* 69(5): 731-735.

Lane, Stout, Hay, Prusak, Hardcastle, Fairchild, et al. (2007) Callophycoic acids and callophycols from the Fijian red alga *Callophycus densus* *J. Org. Chem.* 72(19): 7343-7351.

Lane, Nyadong, Gahlana, Shearer, Stout, Parry, et al. (2009) Desorption electrospray ionization mass spectrometry reveals surface-mediated antifungal chemical defense of a tropical seaweed *Pro. Natl. Acad. Sci. U.S.A* 106(18): 7314-7319.

Ledlie, Graham, Bythell, Wilson, Jennings, Polunin, Hardcastle (2007) Phase shifts and the role of herbivory in the resilience of coral reefs *Coral Reefs* 26(3): 641-653.

Leichter, Stewart, Miller (2003) Episodic nutrient transport to Florida coral reefs *Limnol. Oceano.* 48(4): 1394-1407.

Lewis (1986) The role of herbivorous fishes in the organization of a Caribbean reef community *Ecol. Monographs* 56(3): 183-200.

McManus and Poisenberg (2004) Coral-algal phase shifts on coral reefs: ecological and environmental aspects *Prog. Oceano.* 60(2-4): 263-279.

Mumby and Steneck (2008) Coral reef management and conservation in light of rapidly evolving ecological paradigms *Trends Ecol. Evol.* 23: 555-63.

Mumby (2009) Phase shifts and the stability of macroalgal communities on Caribbean coral reefs *Coral Reefs* 28: 761-773.

Nugues, Smith, Hooidonk, Seabra, Bak (2004) Algal contact as a trigger for coral disease *Ecol. Letters* 7: 919-923.

Nyadong, Hohenstein, Gahlana, Lane, Kubanek, Sherrill, Fernandez (2009) Reactive desorption electrospray ionization mass spectrometry (DESI-MS) of natural products of marine alga *Anal. Bioanal. Chem.* 394: 245-254.

Nylund, Cervin, Hermansson, Pavia (2005) Chemical inhibition of bacterial colonization by *Bonnemaisonia hamifera* *Mar. Ecol. Prog. Ser.* 302: 27-36.

Nylund, Persson, Lindegarth, Cervin, Hermansson, Pavia (2010) The red alga *Bonnemaisonia asparagoides* regulates epiphytic bacterial abundance and community composition by chemical defence *FEMS Mico. Ecol.* 71: 84-93.

Ostrander, Armstrong, Knobbe, Gerace, Skully (2000) Rapid transition in the structure of a coral reef community: The effects of coral bleaching and physical disturbance *Proc. Natl. Acad. Sci. U.S.A* 97(10): 5297-5302.

Paul, Kuffner, Walters, Ritson-Williams, Beach, Becerro (2011) Chemically mediated interactions between macroalgae *Dictyota* spp. and multiple life history stages of the coral *Porites asteroides* *Mar. Ecol. Prog. Ser.* 426: 161-170.

Rasher and Hay (2010) Chemically-rich seaweeds poison corals when not controlled by herbivores *Proc. Natl. Acad. Sci. U. S. A.*, 107, 9683-9688.

Rasher, Stout, Engel, Kubanek, Hay (2011) Macroalgal terpenes function as allelopathic agents against reef corals *Proc. Natl. Acad. Sci. U.S.A* 108(43): 17726-17731.

Ritchie (2006) Regulation of microbial populations by coral surface mucus and mucus-associated bacteria *Mar. Ecol. Prog. Ser.* 322: 1-14.

Rogers and Miller (2006) Permanent 'phase shifts' or reversible decline in coral cover? Lack of recovery of two coral reefs in St. John, US Virgin Islands *Mar. Ecol. Prog. Ser.* 306: 103-114.

Saha, Rempt, Grosser, Pohnert, Weinberger (2011) Surface-associated fucoxanthin mediates settlement of bacterial epiphytes on the rockweed *Fucus vesiculosus* *Biofouling* 27(4): 423-433.

Schmitt, Hay, Lindquist (1995) Constraints on chemically mediated coevolution: multiple functions for seaweed secondary metabolites *Ecology* 76(1): 107-123.

Smith, Shaw, Edwards, Obura, Pantos, Sala, et al. (2006) Indirect effects of algae on coral: algae-mediated, microbe-induced coral mortality *Ecol. Letters* 9: 835-845.

Steinberg, Schneider, Kjelleberg (1997) Chemical defenses of seaweeds against microbial colonization *Biodegradation* 8: 211-220.

Steinberg and deNys (2002) Chemical mediation of colonization of seaweed surfaces *J. Phycol.* 38: 621-629.

Stout, Hasemeyer, Lane, Davenport, Engel, Hay, et al. (2009) Antibacterial neurymenolides from the Fijian red alga *Neurymenia fraxinifolia* *Org. Letters* 11(1): 225-228.

VITA

TIFFANY D. ANDRAS

ANDRAS, was born in Lakeland, Florida. She attended schools throughout Florida and Georgia and received her B.S. from the Georgia Institute of Technology in Applied Biology in 2009, graduating with highest honors. She worked as a laboratory technician and backpacked throughout western Europe before returning to Georgia Tech to pursue a M.A. in aquatic chemical ecology in the Fall of 2010. When she is not working on her research, Ms. Andras loves spending time with her girlfriend and their dog as well as traveling, attending music festivals, being outdoors, and riding her bicycle through the city.